Sánchez-Marín, JR.; Bachiller Martin, MC.; Nova-Giménez, V.; Boria Esbert, VE. (2019). Controlled Out-of-Band Rejection of Filters based on SIW with Alternating Dielectric Line Sections. IEEE Microwave and Wireless Components Letters. 29(4):258-260. https://doi.org/10.1109/LMWC.2019.2902034

Controlled Out-of-Band Rejection of Filters based on SIW with Alternating Dielectric Line Sections

Juan R. Sánchez, Carmen Bachiller, Vicente Nova, and Vicente E. Boria

***Abstract*—A study for managing the out-of-band rejection in a new topology of filters based on Substrate Integrated Waveguide (SIW) with Alternating Dielectric Line Sections (ADLS) is presented in this paper. ADLS is a filtering structure consisting on line sections of the same width but with alternating air and dielectric filling. The design of the lengths of each section provides the central frequency and the bandwidth of a band-pass filter response. The proper selection of the structure substrate dielectric permittivity can increase the rejection band up to $2f_o$. Moreover, the selection of the filter order (i.e. the number of sections with and without dielectric) can affect the depth of the rejection band. A study of width and depth of the rejection band is performed with different permittivities and orders for two different filters. Then, for validation purposes, prototypes of both filters have been manufactured and measured.**

***Index Terms*—alternating dielectric line sections, filter, out-of-band rejection, Substrate Integrated Waveguide (SIW).**

I. INTRODUCTION

IN general, the frequency response (central frequency and bandwidth) of waveguide devices is determined by their dimensions. The insertion of a dielectric material inside the cavities reduces their dimensions, since the electromagnetic field is concentrated within that material. So that, Substrate Integrated Waveguide technology [1] makes the design, manufacturing and integration of microwave devices easier and cheaper, and provides a substantial size reduction. This reduction is related to the dielectric permittivity of the substrate. As a drawback, the substrates are not loss-free, so SIW devices have higher insertion loss than waveguide ones [2].

SIW structures have been successfully employed to implement different bandpass filter topologies, as directly coupled cavities H-plane filters. However, the need of a better performance on passband and stopband, i.e. low insertion loss and wide out-of-band rejection, is increasing.

The insertion loss is limited by the loss tangent of the substrate, and the out-of-band frequency response is limited by the excitation of higher order modes of the filter resonators, which are determined by the topology. The use of Empty SIW (ESIW) technology [3] reduces the insertion loss, but increases the size. Concerning the rejection band, in the case of conventional SIW or ESIW filters, the first spurious is typically located around $1.5f_0$ [2], [3]. Several techniques have been developed to enhance the stopband behaviour [4], [5], but they still have some limitations in the stopband frequency range.

The new filters based on SIW with Alternating Dielectric Line Sections (ADLS) [6] have properties between the ones of SIW and ESIW filters in terms of size and insertion loss. Furthermore, these structures can control the rejection band by changing the dielectric permittivity and/or filter order [7].

II. ALTERNATING DIELECTRIC LINE SECTIONS

ADLS is a topology based on alternating substrate integrated line sections without and with dielectric material, where the empty sections behave as inverters and the filled sections behave as the resonators of a filtering structure. This structure is manufactured on a single substrate, but it needs two metallic covers (up and down) to close the empty sections in order to form the waveguide, thus the final structure is three layered.

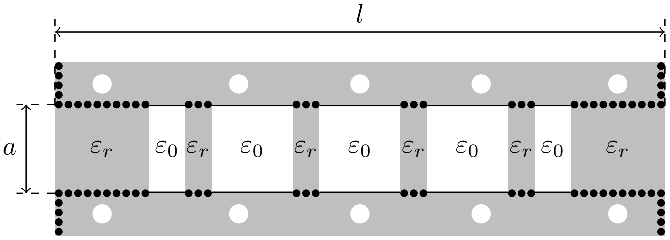

Fig. 1. ADLS filter layout. Black are the metallized vias of the filled sections and the border copper metallization to implement empty sections, gray is the copper metallization on top layer, and white are the empty sections (also metallized on top and bottom) and the fastening screws holes.

TABLE I
DIMENSIONS OF THE BANDPASS FILTERS WITH DIFFERENT SUBSTRATES
(4 POLES, f_0= 11 GHZ, BW= 300 MHZ)

ε_r	Length l (mm)	Width a (mm)	Thickness (mm)
2.2	98.497 ($3.6\lambda_0$)	12.500 ($0.5\lambda_0$)	0.787
3.55	68.379 ($2.5\lambda_0$)	10.500 ($0.4\lambda_0$)	0.813
6	47.170 ($1.7\lambda_0$)	8.000 ($0.3\lambda_0$)	1.270
9.8	34.352 ($1.3\lambda_0$)	6.000 ($0.2\lambda_0$)	1.270

The filter topology is shown in Fig. 1. In the empty sections, the field is confined laterally using metallized walls. In the dielectric sections, metallized via holes, as in the traditional SIW, are used. These vias behave as an electric wall, and they are placed to get an equivalent width equal to the empty sections one [1]. A detailed description of the design strategy of these new filters can be found in [6].

Four bandpass filters have been designed with this technology. They are four-pole Chebyshev filters, with 0.01 dB

The authors are with the Instituto de Telecomunicaciones y Aplicaciones Multimedia, Universitat Politcnica de Valncia, 46021 Valencia, Spain (e-mail: juasncm1@upv.es; mabacmar@dcom.upv.es). This work was partially funded by the Generalitat Valenciana research project PROMETEOII/2015/005, by the Ministerio de Educación, Cultura y Deporte (Spain) under the Fellowship Program for Training University Professors FPU14/00150, and by Ministerio de Economía y Competitividad (Spain) under R&D project TEC2016-75934-C4-1-R.

ripple in the passband, centered at 11 GHz and with 300 MHz of bandwidth, using Rogers substrates with different dielectric permittivity: RT/duroid 5880 with ε_r=2.2, RO4003C with ε_r=3.55, TMM6 with ε_r=6, and TMM10i with ε_r=9.8. The higher the permittivity value, the smaller the size, as can be seen in Table I (the reduction of filter footprint between the biggest and the smallest filters is about 80%). Even when the passband of those realizations is the same, the out-of-band rejection is different depending on the selected permittivity, as can be seen in Fig. 2. The variation of the dielectric permittivity allows to control the width of the rejection band.

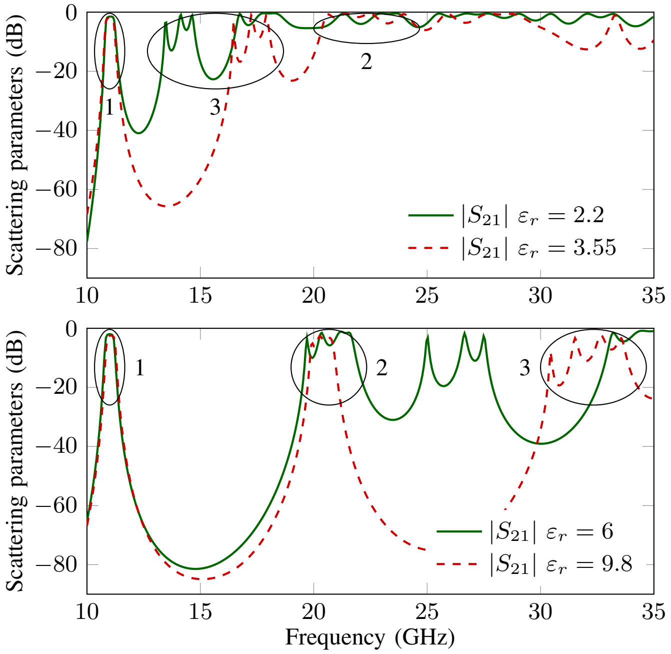

Fig. 2. Simulated frequency response with different dielectric permittivities.

III. STUDY OF THE OUT-OF-BAND BEHAVIOUR

In this section, the width and the depth of the rejected band are studied.

A. *Width of the rejected band.*

In the simulated frequency responses of Fig. 2, different local maxima of the transmission parameters are present, and the reason behind each local maximum is different for each filter. Therefore, a deeper analysis of the electric field inside the filter at those maxima is required to have a clearer idea of the working principle beneath this behaviour.

The frequency response of the filter with ε_r=9.8 is analyzed. The first maximum (circle 1 of Fig. 2) in all the frequency responses is the desired passband of the filter. The electric field at this frequency is shown in Fig. 3(a).

Commonly, the first spurious in a filter appears at the frequency of the second resonant mode of the resonators, whose mode is usually the TE_{102}. The frequency of this mode depends on the resonant section length, permittivity and width. In this particular realization, the inverters are sections of empty waveguides, thus creating a discontinuity. These discontinuities have the effect of reducing the length of the dielectric filled sections, thus increasing the frequency of the second resonance of those sections. This frequency response is represented by circle number 2 in Fig. 2. Its electric field is shown in Fig. 3(b), where the second resonant mode appears in the filled cavities, showing two maxima inside each resonator.

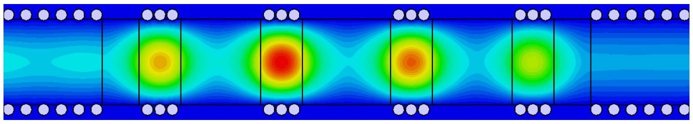

(a) EM field distribution at passband f=11 GHz.

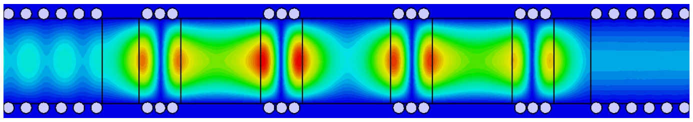

(b) EM field distribution at TE_{102} mode of the resonant section f=20 GHz.

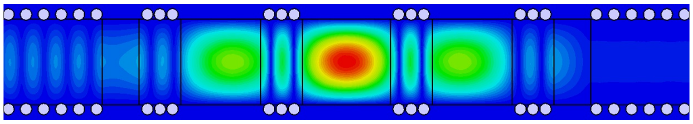

(c) EM field distribution at TE_{101} mode of the inverter f=30.5 GHz.

Fig. 3. EM field distribution for different frequencies of filter with $\varepsilon_r = 9.8$.

Nevertheless, there is another spurious in the rejection band. In this case, the electric field indicates a different working principle: the empty sections propagate at those higher frequencies and concentrate the electric field; they do not behave as inverters but as resonant sections, which mode is TE_{101}. This is shown in Fig. 3(c), where the maxima of the electric field are placed in the empty sections. This mode is represented by circle 3 in all frequency responses of Fig. 2. As it can be seen, this resonance is achieved at different frequencies depending on the substrate permittivity: the lower the permittivity value, the lower the spurious frequency.

Hence, the out-of-band peaks are a combination of the two aforementioned effects, and both can be tuned by the substrate permittivity value. This tuning is limited by two reasons: on the one hand, the change of permittivity modifies the width of the filter and consequently the mode of the empty sections and, on the other hand, the values of dielectric permittivity are conditioned to the available commercial substrates.

B. *Depth of the rejected band.*

The depth of the rejected band is related to the order of the filter, as stated in the study performed in [7]. By increasing the number of the filter sections, the value of that parameter can be increased. In order to asses the versatility of the design strategy, a novel filter centered at 13 GHz with 300 MHz bandwidth and 0.01 dB ripple in the passband is developed. Fig. 4 shows the depth of the rejected band of this filter for 2, 3, 4, 5 and 6 resonant sections. All the filter realizations have been made on the same substrate with ε_r=3.55. As it can be seen, the rejection band is deeper for the higher order filters. It is noticeable that the width of the rejected band is not related to the order of the filter, but to the permittivity value of the

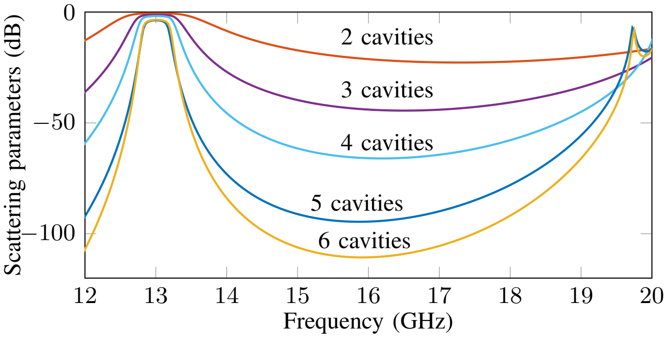

Fig. 4. Impact of the filter order on the depth of the rejected band.

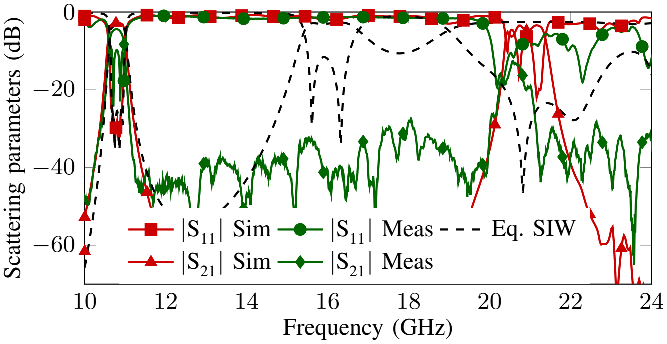

Fig. 5. Comparison between simulated and measured frequency responses for the 4-pole filter with ε_r=9.8.

substrate. With the considered substrate, the second spurious is at $1.5f_0$, no matter the number of resonant sections.

IV. Results

In order to asses the control of the out-of-band response, two of the previously designed filters have been manufactured. The 11 GHz filter was manufactured with substrate TMM10i, ε_r=9.8 and $tan\delta$=0.0020. The simulated and measured frequency responses are in Fig. 5. Additionally, the 13 GHz filter has been manufactured with RO4003C substrate, ε_r=3.55, and $tan\delta$=0.0027. The 5-poles case has been selected, which frequency response is shown in Fig. 6.

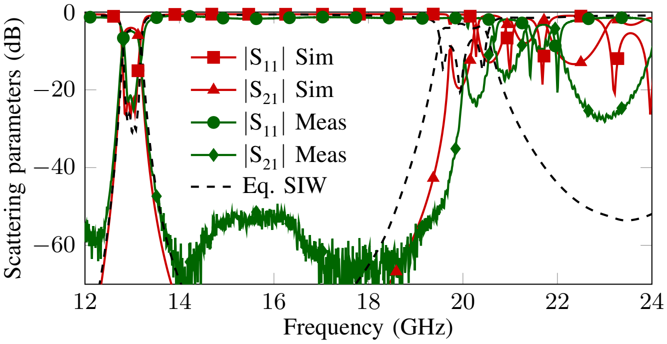

Fig. 6. Comparison between simulated and measured frequency responses for the 5-pole filter with ε_r=3.55.

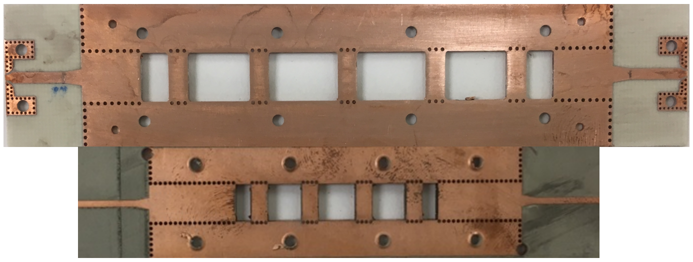

Fig. 7. Manufactured filters. On top, 13 GHz and 5 cavities filter with RO4003C. Bottom, 11 GHz and 4 cavities filter with TMM10i.

In both cases, the simulated and measured results show a good agreement. The measured insertion loss is higher due to the effect of transitions and connectors. The 13 GHz filter has insertion and return loss of values equal to 4 dB and 25 dB, respectively. In the 11 GHz case, the insertion loss is around 3 dB due to the substrate features and reduced center frequency. However, a misalignment between simulated and measured return loss, of 30 dB and 10 dB respectively, can be observed. This is caused by the type of employed connectors. The 13 GHz filter uses screwed End-Launch with enhanced performance, while in the case of 11 GHz filter the height of the substrate forced to employ typical welded SMA (see the footprint of both filters in Fig. 7).

Furthermore, the frequency responses of equivalent SIW filters with the same features (in terms of central frequency, bandwidth, substrate and order) have been included in Fig. 5 and 6, with the aim of confirming the expected results for the out-of-band behaviour.

V. Conclusion

A study of the rejected band of ADSL filters has been conducted. This study shows that the width of the rejected band can be controlled by the substrate permittivity value, up to $2f_0$. Moreover, its depth can be controlled by the filter order. The results show that the conclusions are consistent for different frequencies, substrates and filter orders.

References

[1] D. Deslandes and K. Wu, "Integrated microstrip and rectangular waveguide in planar form," *IEEE Microw. Wireless Compon. Lett.*, vol. 11, no. 2, pp. 68–70, Feb 2001.

[2] X. Chen and K. Wu, "Substrate integrated waveguide filters: Design techniques and structure innovations," *IEEE Microw. Magazine*, vol. 15, no. 6, pp. 121–133, Sept 2014.

[3] A. Belenguer, H. Esteban, and V. E. Boria, "Novel empty substrate integrated waveguide for high performance microwave integrated circuits," *IEEE Trans. Microw. Theory and Techn.*, 2014.

[4] X. Chen, K. Wu, and D. Drolet, "Substrate integrated waveguide filter with improved stopband performance for satellite ground terminal," *IEEE Trans. Microw. Theory Techn.*, vol. 57, no. 3, pp. 674–683, March 2009.

[5] T. Huang, X. Yang, Y. Huang, Z. He, and Z. Shao, "An X-band SIW-DGS bandpass filter with improved stopband performance," in *2015 IEEE Int. Conf. Commun. Problem-Solving (ICCP)*, Oct 2015, pp. 473–474.

[6] J. R. Sánchez, C. Bachiller, M. Juliá, V. Nova, H. Esteban, and V. E. Boria, "Microwave filter based on substrate integrated waveguide with alternating dielectric line sections," *IEEE Microw. Wireless Compon. Lett.*, vol. 28, pp. 990–992, Nov 2018.

[7] L. Silvestri, E. Massoni, C. Tomassoni, A. Coves, M. Bozzi, and L. Perregrini, "Substrate integrated waveguide filters based on a dielectric layer with periodic perforations," *IEEE Trans. Microw. Theory Techn.*, vol. 65, no. 8, pp. 2687–2697, Aug 2017.